Diffusional Film Characteristics in Turbulent Flow: Dynamic Response Method

John J. Keyes, Jr.
Union Carbide Nuclear Company, Oak Ridge, Tennessee

Application of a dynamic or unsteady-state technique to the problem of radial mixing in a tube is described. Measurement of the amplitude attenuation suffered by a sinusoidally modulated gas composition wave as it flows within an open (unpacked) tube makes possible the direct determination of an "equivalent gas film thickness" from which a mass transfer film coefficient may be readily calculated.

A brief summary of the method employed for obtaining the necessary mathematical relationships is presented, along with descriptions of the techniques developed for measurement of small amplitude differences at wave frequencies as high as 10 cycles /sec.

Experimentally, conditions were varied to include a range of Schmidt number from 0.18 to 1.24 and of Reynolds number from 4,000 to 50,000. The results of this work appear to fall nearly in line with the semitheoretical equation of Martinelli as written for mass transfer. Generally speaking, α was found to be an increasing function of N_{Sc}, varying from about 0.5 to a maximum of 0.77; β, in turn, was found to increase with N_{Re} from 0.3 to 0.5.

A suggestion for extending the method to measurement of eddy diffusivities in the axial direction is included.

The fact that transfer of material between a flowing gas stream and an interface does not take place instantaneously is of prime significance in the design of equipment for separation and purification of fluid mixtures. Consequently, much work has been done, both theoretically and experimentally, to ascertain the dependence of mass transfer rates on measurable quantities, such as gas properties and flow rates. The dynamic or unsteady-state method(*7*) shows promise as a new research tool for investigation of these and other fundamental problems. It is the intent of this paper to present the basic theory and to describe experimental techniques as developed for application of the method to mass transfer in open tubes, together with some preliminary data which seem to bear out the validity of the method. It is felt, further, that the techniques here described are applicable in general to other problems where the dynamic method might be contemplated.

The method makes use of the fact that a fluid stream which has a cyclically varying composition undergoes a decrease in amplitude and a corresponding phase shift by virtue of radial mass transfer. To visualize the mechanism involved one may find it helpful to consider the combined resistance to transfer by both eddy and molecular diffusion as lumped into an "equivalent" diffusional film of such thickness, B_F, that the entire concentration gradient between gas and interface would be just sufficient to cause *molecular* diffusion through the film at the proper rate. The influence of the cyclic composition variation, then, is to impose a fluctuating radial concentration gradient, the effect of which in combination with the hold-up or "capacity" of the gas film is to smooth out the variations and to introduce some phase shift as the wave progresses down the tube.

The experimental procedure consists in comparing amplitude, and where necessary, phase of the outlet with that of the inlet stream. From these measurements it is possible by application of the appropriate functional relationships to determine the equivalent gas film thickness, and herefrom the film coefficient, k_g, directly. No measurement of compositions within the tube need be made, and in contrast to wetted-wall techniques no liquid phase is required. This latter feature makes the dynamic method particularly well suited for studies on noncondensable gas pairs.

PREVIOUS WORK

The cyclic method was employed by Bell and Katz(*1*) to determine surface heat transfer coefficients by utilizing sinusoidal temperature input. Later Dayton et al.(*2*) by an improved method obtained good agreement with conventional heat transfer data for several geometries.

The original application to mass transfer was made by Rosen and Winsche(*5*), who investigated rate processes in absorption beds with sine wave input.

Perhaps the most lucid exposition of the method is that of Deisler(*3*), who extended the theory to a determination of three independent rate mechanisms and applied the results to diffusion in a packed bed. Indeed, it was Deisler's work which suggested the application of the dynamic method to the problem considered here.

APPARATUS AND INSTRUMENTATION

The dynamic response method requires a means for generating the sinusodial composition wave at constant total flow rate and pressure together with a means for measuring the wave amplitude and phase. Frequencies in the range from 3 to

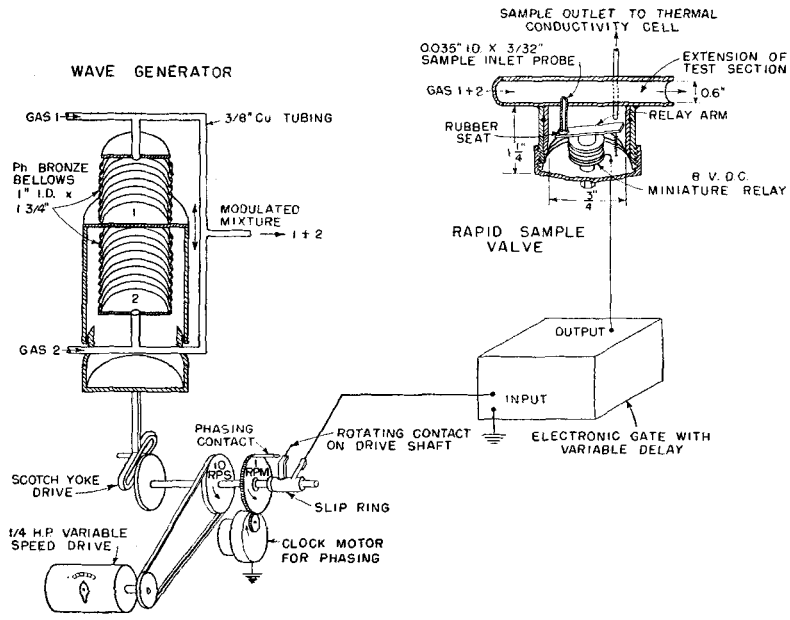

Fig. 1. Diagram of apparatus.

10 cycles/sec. are required, depending on conditions, to give measurable attenuation.

Figure 1 includes a sketch of the wave generator. It consists of a pair of matched bellows mounted rigidly at the ends and separated by a movable central partition, the latter being attached to a scotch-yoke drive mechanism to give reciprocating motion. Each bellows chamber communicates directly with a gas supply line as indicated. Because of push-pull action of the bellows, pressure and flow variations are canceled, giving as output the pure composition function desired. Operation as high as 15 cycles/sec. is feasible with this design, maintaining reasonably good wave form.

Analysis of the modulated wave is basically by thermal conductivity; however direct, continuous sampling from the test section through the thermal element proved unsatisfactory. Even with a specially designed rapid-response cell, short lines, and low pressure, the output signal was found to fall off rapidly above 1 cycle/sec., mainly because of mixing in the sample lines and chambers. Figure 2 is a block diagram of the apparatus as finally developed, capable of responding to as high as 10 cycles/sec. but utilizing only standard thermal conductivity cells and recorder. This scheme enables simultaneous measurement of attenuation and phase shift.

The test section consists of an 8-ft. length of glass tubing, 0.61 in. I.D., preceded by a 6-ft. entrance section and an expanded section of open pipe for attenuation of any harmonics present in the generated wave. Two relay operated rapid sampling valves are provided at either end of the test section for the purpose of monitoring the gas wave. These valves act to withdraw a small volume of sample gas when energized for a predetermined fraction of a cycle (2 to 5%) by means of the rotating contact on the generator shaft. Provision for delaying (or advancing) the action of valve B with respect to valve A is provided by an electronic delay gate variable from 0 to 250 msec.

Operation of the sampling system can best be understood by reference to Figure 3. If points indicated by x represent withdrawal of a sample at each cycle of the fundamental wave at some arbitrary time, the output of the valve is a constant gas composition with magnitude depending on the relationship in phase (or time) between the wave generator stroke and the signal to the sampling relay. To obtain a complete representation of the wave it is necessary simply to scan through 360° by continually rotating the phase of the synchronizing contact with respect to the generator shaft. Thus, the sampling point is made to traverse the wave, as indicated by the points marked •, at sufficiently low frequency for the analytical system to follow. The over-all result is a reproduction of the original wave in amplitude and phase but at greatly reduced frequency. A scanning rate of about 1 cycle/min. is satisfactory. Figure 4 is the trace of a typical wave form so obtained. Figure 1 shows an isometric view of the relay valve and scanning mechanism. Figures 5 and 6 are, respectively, photographs of the wave generator and of the over-all apparatus.

The method of determining attenuation and phase is straightforward. Outputs of the two samplers, at 7 cm. Hg, flow to opposite sides of a thermal conductivity bridge (Gow-Mac Company, NRL Model), the output of which depends on amplitude and phase relationships of the two input waves. If these are

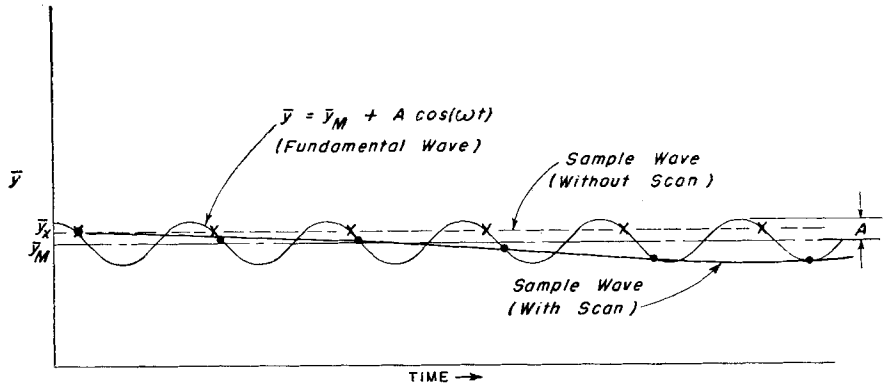

Fig. 3. Operation of the rapid sampling system, illustrating reduction in output frequency.

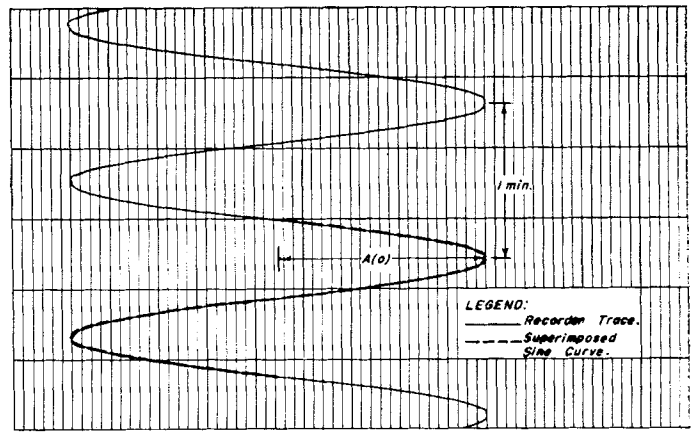

Fig. 4. Typical wave trace; fundamental frequency, 7 cycles/sec.

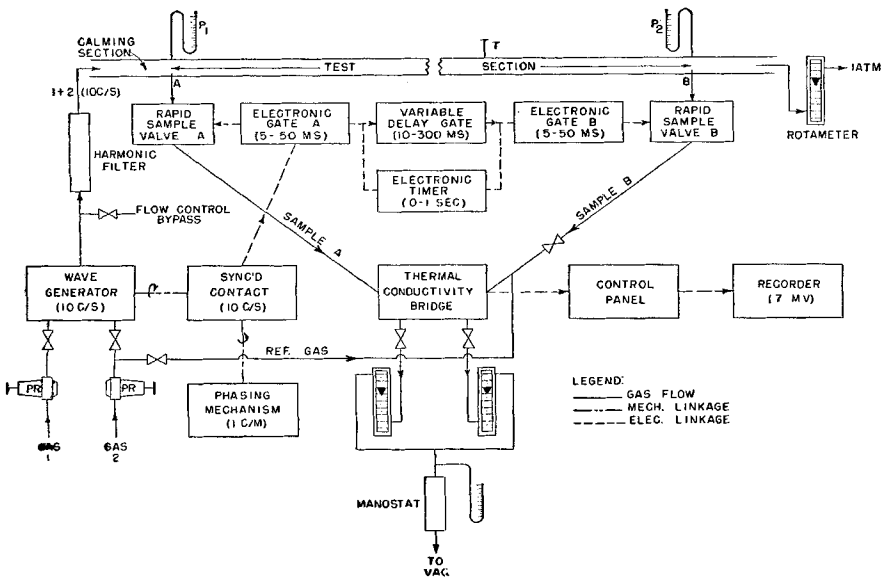

Fig. 2. Block diagram of apparatus.

Fig. 5. Wave generator and phasing mechanism.

exactly in phase, a sensitive recorder connected across the bridge will indicate amplitude difference directly. Thus, when the variable delay on B is adjusted for minimum output amplitude, which will approach a true null as $A(L) \rightarrow A(O)$, the two sample waves are in phase, and the delay as read on the timer is a measure of the phase lag between the sample points. The attenuation ratio of the wave

$$\frac{A(L)}{A(O)} = 1 - \frac{A(O) - A(L)}{A(O)}$$

is obtained from the indicated amplitude difference and the initial amplitude $A(O)$.

ANALYTICAL TREATMENT AND DISCUSSION

An understanding of the mechanism by which equivalent film thickness is related to attenuation and phase shift of the sinusoidal composition wave can best be attained by consideration of the behavior of the wave with reference to its radial and longitudinal travel. Attention is here confined to the case of an open (unpacked) tube through which the gas is flowing.

As indicated in the introductory remarks, use is made of the equivalent gas film concept in the analysis. This simplifying approach is probably adequate provided consistency in the definition of the transfer coefficient is maintained. Accordingly, the gas film coefficient, k_g, is related to film thickness, B_F, as follows:

$$k_g = \frac{\rho D}{B_F} \qquad (1)$$

where ρ and D are respectively gas density and molecular diffusivity. Equation (1) is simply the expression of Fick's law for equimolar, countercurrent diffusion. Since the experimental measurements yield values for B_F directly, as will be seen, it was decided to report the results in terms of the latter quantity, with the understanding that the mass transfer coefficient which would obtain for a given N_{Re} and N_{Sc} is directly calculable from Equation (1).

The interior of the tube of diameter d is divided into a central turbulent core of uniform radial composition y and constant mass velocity G, based on the inside tube area, and a peripheral nonturbulent film of thickness B_F, uniform velocity V (the assumption of uniform velocity in the film being necessary to obtain a solution in closed form), and varying radial composition y, as indicated in Figures 7 and 8. As the gas wave progresses along the tube, there is exchange by diffusion between the core and film, the net result of which is equivalent to mixing of the components of the wave (amplitude reduction) and lagging behind of the wave crests (phase shift). Note that there is no net radial flow. only transient flow alternately toward and away from the wall. In addition, there may also be mixing in the axial direction, depending on the magnitude of the longitudinal eddy diffusion coefficient, D_L, and the concentration gradient. It is desired to obtain a quantitative expression for the relationships among these variables.

The differential material balance over a cylindrical core volume element in the direction of flow is first written (*see* **Figure 7**):

Core Equation

$$\frac{4N(1+2B_F/d)}{d} + \frac{V_M}{\bar{V}}\left(G\frac{\partial \bar{y}}{\partial z} - D_L\rho\frac{\partial^2 \bar{y}}{\partial z^2}\right) + \rho\frac{\partial \bar{y}}{\partial t} = 0 \qquad (2)$$

N is the rate of transport of one component from the core to the film, based on the inside film perimeter and evaluated at $x = B_F$. $V_M/\bar{V}$, the ratio of maximum to average velocity, depends on the particular choice of the film velocity, V:

1. $V=0$: $V_M/\bar{V} \cong 1 + 4\frac{B_F}{d}$
2. $V = V_M/2$: $V_M/\bar{V} \cong 1 + 2\frac{B_F}{d}$
3. $V = V_M$ $V_M/\bar{V} \cong 1$

N is obtained from an independent material balance across the film (*see* Figure 8):

Film Equation

$$V\frac{\partial y}{\partial z} + D\frac{\partial^2 y}{\partial x^2} + \frac{\partial y}{\partial t} = 0 \qquad (3)$$

Obviously,

$$N = Dp\frac{\partial y}{\partial x}\bigg|_{x=B_F} \qquad (4)$$

Boundary conditions for (3) are

$$\frac{\partial y}{\partial x}\bigg|_{x=0} = 0 \qquad (5)$$

$$y = \bar{y}\bigg|_{x=B_F} \qquad (6)$$

It is desired to obtain a solution of (2) at $z = L$, subject to the harmonic boundary condition at the inlet, $z = 0$:

$$\bar{y} = \bar{y}_M + A(O)\cos\omega t \qquad (7)$$

Equations (2) and (3) can be readily solved by the method of separation of variables, if the coefficients V, ρ, D, D_L, etc., are as-

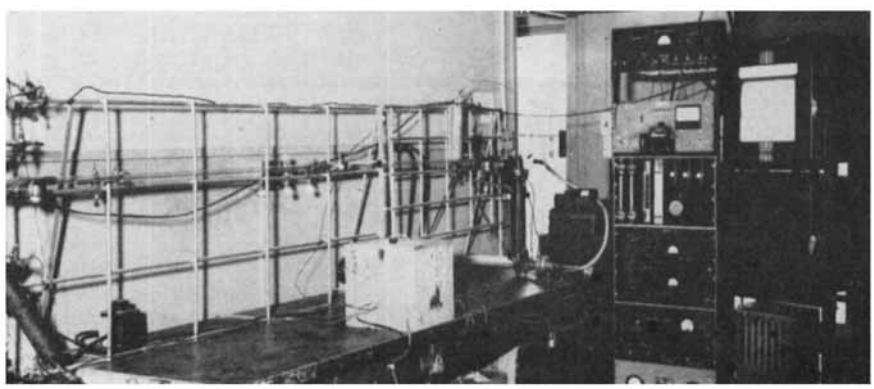

Fig. 6. Over-all view of the apparatus.

sumed to be constants,* and exp $(i\omega t)$ is taken as the time dependent factor, a consequence of (7). In the final step imaginary terms are dropped, and a solution to (2) of the following form is reached:

$$\bar{y}(z) = \bar{y}_M + A(O)\exp[-R(z)]\cos[(\omega t - \phi(z)] \quad (8)$$

$$\therefore \frac{A'(L)}{A(O)} = \exp[-R(L)] \text{ attenuation ratio} \quad (9)$$

R, the attenuation exponent, and ϕ, the phase shift, are functions of known quantities G, ρ, D, etc., and of B_F, which is to be determined. Solutions have been obtained for the three assumed film velocities already discussed. The result for R is essentially independent of V, and one may conclude that knowledge of the velocity profile is *not* necessary so far as amplitude measurements are concerned. Since, on the other hand, ϕ does exhibit a strong dependence on assumed velocity distribution, it was decided to base all results on the attenuation measurements and to leave for a possible future program the interpretation of phase shift data.

*This is essentially true for small amplitudes, say, <10%.

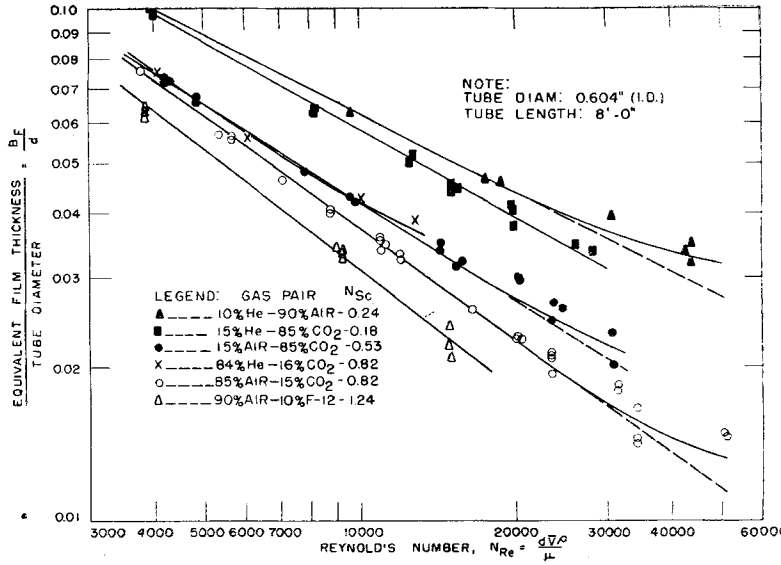

Fig. 9. Summary of experimental results: $-\frac{B_F}{d}$ vs. N_{Re}

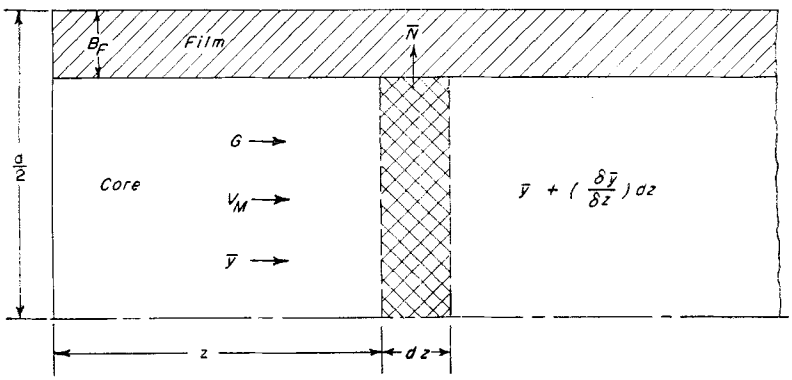

Fig. 7. Nomenclature for core equation.

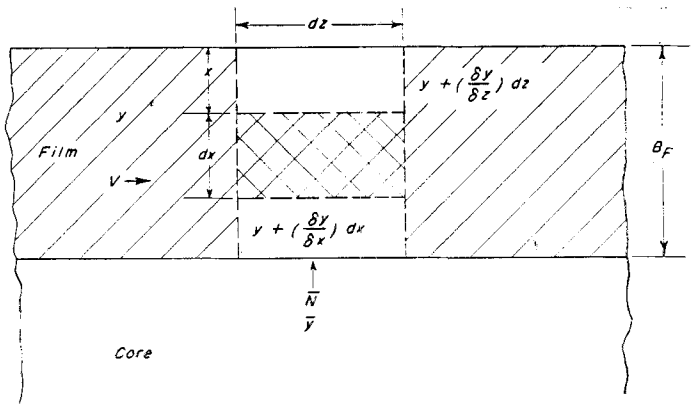

Fig. 8. Nomenclature for film equation.

Attenuation Exponents

Case 1. Longitudinal diffusion is negligible in comparison with radial diffusion.

This situation obtains normally, since longitudinal concentration gradients are very much smaller than the radial gradients. (Wave lengths of the order of 2 to 10 ft. were employed in this work.) Hence, the second order term in (2) is dropped:

$$R(L) = \frac{2\rho L(2\omega D)^{\frac{1}{2}}\left(1 - \frac{2B_F}{d}\right)}{dG}\left[\frac{\sinh\gamma - \sin\gamma}{\cosh\gamma + \cos\gamma}\right]$$

where $\gamma =$

$$\left(\frac{2\omega}{D}\right)^{\frac{1}{2}} B_F \quad (10)$$

When γ is sufficiently small that the hyperbolic and trigonometric functions can be represented by their respective series with only first and third degree terms included, the preceding result simplifies considerably:

$$R(L) \cong \frac{4\rho L\omega^2 B_F{}^3 (1 - 2B_F/d)}{3dGD} \quad (10a)$$

Equation (10a) holds to within about 1% when solved for B_F, with γ as great as 1.0. It is apparent that the attenuation will be a strong function of frequency and of film thickness in particular. The method is therefore quite sensitive for determination of the latter quantity.

Case 2. Perfect radial mixing is assumed and $B_F = 0$ is set in Equations (2) and (3), only the longitudinal mixing effect being left.

For this case

$$R'(L) = \frac{\rho^3 \omega^2 L D_L}{G^3} \quad (11)$$

Some notion of the magnitude of the longitudinal effect can be obtained by substitution of typical values in Equation (11):

$V = G/\rho = 28$ ft./sec. (corresponding to $N_{Re} \cong 10{,}000$ in 0.6-in. I.D. tube)

$\omega = 2\pi f = 24$/sec.
$D_L = D = 1.8\times10^{-4}$ sq.ft./sec. (air-CO_2)
$L = 8$ ft.,
giving

$$\left.\frac{A(L)}{A(O)}\right|_{\text{axial mixing}} = \exp(-R') = 0.9995$$

Even though D_L were 100 times as great as D, which might possibly be true at very high N_{Re}, the effect of longitudinal diffusion is probably negligible as assumed, since under these same conditions

$$\left.\frac{A(L)}{A(O)}\right|_{\text{radial mixing}} \simeq 0.9.$$

EXPERIMENTAL CONSIDERATIONS AND RESULTS

Film thickness determinations covering a wide range of Reynolds and Schmidt numbers were desired. Because of their availability and sensitivity to analysis by thermal conductivity, the following gas pairs were employed:

Gas pair	Light comp., %	μ cp.	ρ, lb./cu. ft.	D, sq. ft./sec.	N_{Sc}
He-CO_2	15	1.61×10^{-2}	9.76×10^{-2}	6.2×10^{-4}	0.18
He-Air	10	1.81	6.76	7.5	0.24
Air-CO_2	15	1.50	10.72	1.77	0.53
Air-CO_2	50	1.61	9.36	1.77	0.65
He-CO_2	84	1.85	2.67	6.2	0.82
Air-CO_2	85	1.73	8.02	1.77	0.82
Air-Freon-12	90	1.73	9.88	0.95	1.24

(values given at 25°C., 1 atm.)

Reynolds numbers were varied from about 4,000 to 50,000 for the 85% air–15% CO_2 system; the upper limit for the other systems was 20,000 to 30,000.

Because of difficulty in interpretation of the phase shift measurements, as well as some uncertainties in the data, discussion of this portion of the work has been omitted.

Typical amplitude data for 85% air–15% CO_2 are listed in Table 1. Repeat runs at approximately constant N_{Re} but varying frequency are included for the purpose of ascertaining any second-order frequency dependence. In addition, some runs at varying initial amplitude, $A(O)$, were made to detect possible nonlinearity. Results of the attenuation measurements are summarized in Figure 9.

Discussion of the Results

Logarithmic plots of B_F/d vs. N_{Re}, with N_{Sc} as parameter, Figures 9 and 10, are suggested by conventional mass transfer correlations of the form

TABLE 1.—TYPICAL DYNAMIC RESPONSE AMPLITUDE DATA

15% CO_2—85% Air (N_{Sc}=0.82)
Tube length L=8.03 ft.
Tube diameter $d=5.07\times10^{-2}$ ft.
Temperature: approx. 25°C.
Pressure: approx. 1 atm.

Run number	Flow rate, cu. ft./min. 25°C. 1 atm.	Frequency, cycles/min.	Initial amplitude $A(O)$, %	Measured attenuation $\frac{A(L)}{A(O)}$	N_{Re}	γ	$\frac{B_F}{d}$ from Eq. (11)
11	1.310	162	7.6	0.409	3770	1.402	0.0760
25a	1.850	208	6.2	0.592	5330	1.240	0.0566
12a	1.956	161	5.6	0.739	5640	1.082	0.0556
b	1.956	211	6.5	0.613	5640	1.227	0.0553
83	2.44	206	8.0	0.801	7080	1.005	0.0462
13a	3.035	202	5.5	0.872	8750	0.913	0.0397
b	3.035	290	7.1	0.742	8750	1.127	0.0407
24c	3.81	251	5.6	0.886	10960	0.918	0.0358
b	3.81	291	6.5	0.874	10960	0.928	0.0339
a	3.81	363	7.6	0.794	10960	1.077	0.0352
82	3.85	205	—	0.936	11100	0.775	0.0346
14	4.10	273	6.5	0.886	11820	0.925	0.0347
10a	4.10	275	7.8	0.895	11820	0.888	0.0323
c	4.10	323	6.0	0.838	11820	1.018	0.0328
23d	5.73	246	—	0.969	16450	0.668	0.0259
a	5.73	363	—	0.905	16450	0.910	0.0280
80	6.93	231	6.0	0.984	20100	0.570	0.0229
79	6.95	307	6.0	0.968	20150	0.680	0.0228
78	7.56	382	—	0.962	21900	0.720	0.0228
17a	8.10	321	6.0	0.977	23500	0.640	0.0209
22	8.10	323	5.0	0.977	23500	0.640	0.0213
15d	8.10	329	5.0	0.981	23500	0.660	0.0193
18c	8.10	382	5.6	0.955	23500	0.786	0.0235
15b	8.10	470	8.5	0.930	23500	0.888	0.0241
73	10.84	261	4.0	0.9930	31400	0.495	0.0182
74	10.91	335	5.2	0.9875	31500	0.574	0.0186
27a	11.75	303	4.6	0.9948	34100	0.442	0.0145
b	11.75	341	5.2	0.9903	34100	0.535	0.0166
d	11.75	494	6.9	0.970	34100	0.740	0.0193
81a	17.45	383	—	0.9941	50500	0.505	0.0149
76	17.60	415	5.2	0.9928	51000	0.532	0.0147

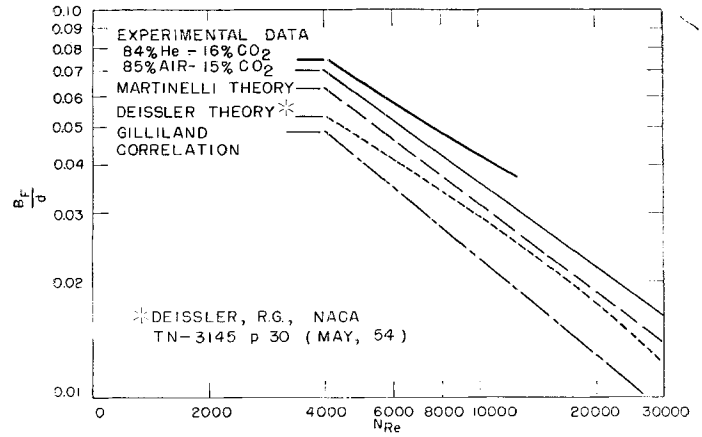

Fig. 10. Comparison of theory and experiment for $N_{Sc} = 0.82$.

$$B_F/d = k N_{Re}^{-\alpha} N_{Sc}^{-\beta} \quad (12)$$

A dependence on a Reynolds number of this form does indeed seem to fit the experimental results for $N_{Re}<20{,}000$, with α an increasing function of N_{Sc} as indicated in Figure 11. At high N_{Re}, however, there is some apparent leveling off of the dependence, attributable possibly to certain experimental difficulties:

1. At the higher flow rates there appears to be a small **frequency** effect, as shown in Table 1, tending to raise the film thickness as frequency is increased at constant N_{Re}. This effect may be due in part to increased wave distortion.

2. Spread in the results for B_F/d at constant N_{Re}, increasing at the higher flow rates, may be attributed also to exaggeration of random errors, a consequence of the increased sensitivity required to measure smaller and smaller amplitude differences.

3. Longitudinal mixing may contribute to the observed attenuation at high N_{Re}, although this seems unlikely.

It might be pointed out, on the other hand, that variation in initial amplitude $A(O)$ from 2% to 8% had no significant effect on the results. (This conclusion might have to be qualified under extreme conditions, such as the case of a high proportion of He in CO_2, where gas density changes significantly with composition.)

Figure 12 illustrates the observed dependence on Schmidt number at constant Reynolds number. In this case the data do not indicate a linear relationship over the entire range of N_{Sc} as ordinarily assumed. Only at the high range, say $0.6<N_{Sc}<1.2$, could one interpret such a relationship to hold. Figure 13 illustrates the observed variations in slope, $-\beta$, based on the above limited range, with N_{Re}.

Comparison with Theory

It is apparent from the variation in slopes of both N_{Re} and N_{Sc} diagrams that the simplest form of Equation (12), obtained by assuming constant exponents, does not represent the results here reported. Some previous work with the equation of Martinelli(*4*), as written for mass transfer, had been encouraging; consequently, it was decided to compare the results with this semitheoretical equation:

$$\frac{B_F}{d} = \frac{32.95 R_c [\alpha N_{Sc} + \ln(1+5\alpha N_{Sc}) + \frac{1}{2}\ln 2.53\times10^{-3} N_{Re}^{0.9}]}{\alpha N_{Sc} N_{Re}^{0.9}} \quad (13)$$

R_c is the ratio of mean to maximum concentration difference. Equation (13) was derived from a more general form of the equation as given by Sherwood and Pigford(*6*) by substitution of the simplified Blasius friction factor expression

$$f = \frac{0.046}{N_{Re}^{0.2}}$$

The value of the parameter

$$\alpha \left(= \frac{\epsilon H}{\epsilon M} \right)$$

was taken as 0.9, based on a comparison of some earlier data.

Comparison of the results with Equation (13) is included in Figures 10 and 11. The Martinelli

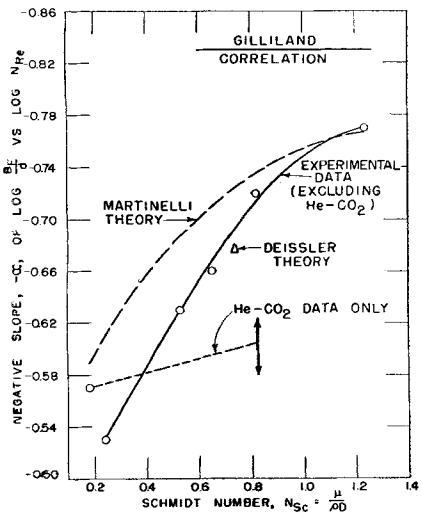

Fig. 11. Schmidt-number dependence of Reynolds-number exponent, $-\alpha\left(\frac{B_F}{d} = K N_{Re}^{-\alpha} N_{Sc}^{-\beta}\right)$.

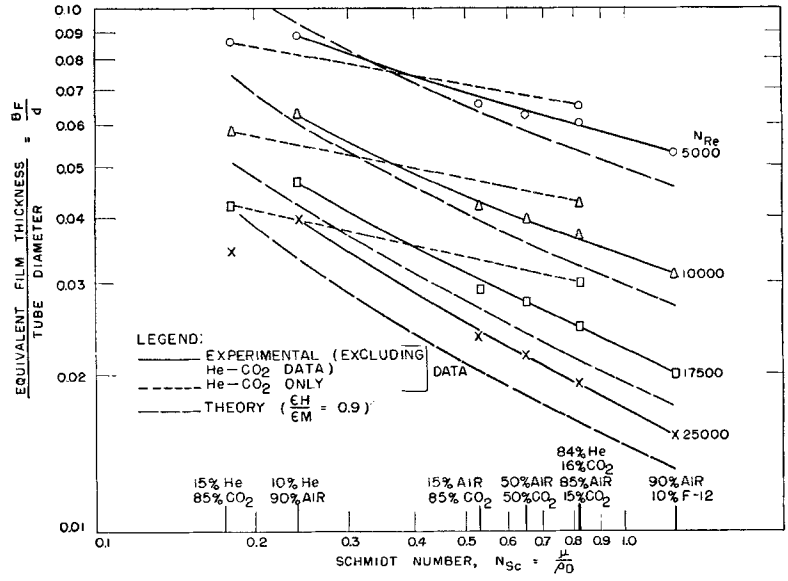

Fig. 12. Comparison of results with Martinelli theory: $\frac{B_F}{d}$ vs. N_{Sc}.

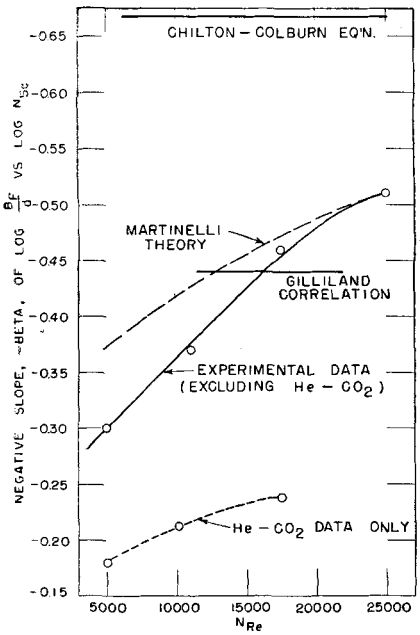

Fig. 13. Reynolds number dependence of Schmidt number exponent, $-\beta$, for $0.6 < N_{Sc} < 1.24$ $\left(\frac{B_F}{d} = KN_{Re}^{-\alpha}N_{Sc}^{-\beta}\right)$.

equation plots nearly linearly with N_{Re} at constant N_{Sc}, over the range of interest, falling a little below the measured results. Note that the experimental and theoretical slopes, $-\alpha$, compared in Figure 11, exhibit similar variations with N_{Sc}, with particularly good agreement for $N_{Sc} > 0.8$.

Figure 12 is a further comparison of results with Equation (13). B_F/d is considered a function of N_{Sc} at constant N_{Re}. The anomalous behavior of He-CO_2 is observed in Figure 10 as a lack of agreement with air–CO_2 data at the same Schmidt and Reynolds numbers and is evidenced further by the abnormally low N_{Re} and N_{Sc} dependence (Figures 11 and 13). These effects are not at present understood.

Variations in experimental and theoretical slopes, $-\beta$, with N_{Re}, as plotted in Figure 13, show surprising similarities. There seems to be a leveling off in β with increasing N_{Re} toward a value somewhat above 0.44 obtained by Gilliland.

An interesting potentiality of the dynamic method for measurement of axial eddy diffusivity in open tubes exists, for it can be shown that phase shift of the modulated wave should occur independently of longitudinal mixing. From simultaneous measurements of attenuation and phase, therefore, D_L may be determined. Difficulty in obtaining and interpreting phase measurements has thus far prevented attainment of this end.

Discussion of Experimental Errors

Aside from ever-present errors, such as those in calibration and flow metering, certain difficulties associated with generation and detection of the modulated wave might be mentioned. Wave distortion may be introduced at the generator by bellows mismatch, play in bearings and yoke, excessive pressure differences between bellows, etc. If not too serious, such distortions can be removed by the expanded tube filter, which attenuates the higher order harmonics.

The rapid sampling technique in itself may introduce apparent wave distortion, particularly if the phasing rate is too great compared with the fundamental frequency or if the sampling time is too long. In general, the phasing frequency should not exceed 0.5% of the fundamental, and the sampling time 5% of a cycle. Figure 4, previously discussed, illustrates the good sinusoidal wave form attainable.

CONCLUSION

The dynamic response method shows promise as a tool for fundamental studies related to gas mixing and mass transfer, where conventional methods are unwieldy or in some cases inapplicable. The work described here is an illustration of the sensitivity and flexibility of the method and of the nature of experimental techniques found applicable to the specialized problems of generating and monitoring a high frequency gas composition wave. Experimental evidence of deviations from the commonly utilized mass transfer correlations is discussed. Because of the preliminary nature of the results, no attempt to present a specific correlation of the data has been made other than to point out the similar trend to that predicted by the semitheoretical Martinelli equation.

ACKNOWLEDGMENT

The author wishes to express appreciation to G. A. Kuipers, for suggesting the design of the wave generator, to D. F. Smith for the basic idea of rapid sampling, and to J. H. Lykins and H. S. McKown for design and for development of the electronic equipment.

NOTATION

A = interfacial area, sq. ft.
$A(L)$ = amplitude at distance L from inlet
$A(O)$ = amplitude at inlet
B_F = equivalent film thickness, ft.
d = inside tube diameter, ft.
D = molecular diffusivity, sq.ft./sec.
D_L = longitudinal (eddy) diffusivity, ft./sec.
f = friction factor
G = axial mass velocity, lb./(sec.)(sq.ft.)
k_g = gas film transfer coefficient, lb./(sec.)(sq.ft.)(mole fraction)
K_g = over-all gas film mass transfer coefficient, lb./(sec.)(sq. ft.)(mole fraction)
L = tube length, ft.
N = radial mass velocity of one component, lb./(sec.)(sq.ft.)
N_{Re} = Reynolds number, $d\overline{V}\rho/\mu$
N_{Sc} = Schmidt number, $\mu/\rho D$
$R(L)$ = radial attenuation exponent
$R'(L)$ = axial attenuation exponent
R_c = ratio mean to maximum Δy
t = time, sec.
V = velocity of film, ft./sec.
$\overline{V}$ = average velocity, ft./sec.
V_M = maximum velocity, ft./sec.
W' = radial mass rate of diffusing component, lb./sec.
x = radial distance from tube wall, ft.
y = film concentration
$\overline{y}$ = core concentration
$\overline{y_M}$ = mean core concentration
z = distance from tube inlet, ft.

Greek Letters

α = Reynolds number exponent, also $\alpha = E_H/E_M$ (= eddy diffusivity for heat or mass/eddy diffusivity for momentum)
β = Schmidt number exponent
$\gamma = (2\omega/D)^{\frac{1}{2}}B_F$
μ = mean viscosity, lb./(ft.)(sec.)
ρ = mean density, lb./cu.ft.
ϕ = phase shift
ω = angular frequency, radian/sec.

LITERATURE CITED

1. Bell, J. C., and E. F. Katz, "Heat Transfer and Fluid Mechanics Institute," Am. Soc. Mech. Engrs., Berkeley, Calif. (June 22, 1949).
2. Dayton, R. W., et al., *Rept. BMI-747*, Battelle Memorial Institute (1952).
3. Deisler, P. F., Jr., Ph.D. Dissertation, Princeton University (June, 1952).
4. Martinelli, R. C., *Trans. Am. Soc. Mech. Engrs.* 69, 947-959 (1947).
5. Rosen, J. B., and W. E. Winsche, *J. Chem. Phys.*, 18, 1587 (1950).
6. Sherwood, T. K., and R. L. Pigford, "Absorption and Extraction," 2 ed., p. 63, McGraw-Hill Book Company, Inc., New York (1952).
7. Wilhelm, R. H., *Chem. Eng. Progr.*, 49, No. 3, 153 (1953).